Running Head: Force control strategies following ACL reconstruction

Neuroplastic alterations in common synaptic inputs and synergistic motor unit clusters controlling the vastii muscles of individuals with ACL reconstruction

Stefano Nuccio [1], Carina M. Germer [2,3], Andrea Casolo [4], Riccardo Borzuola [1], Luciana Labanca [5], Jacopo E. Rocchi [6], Pier Paolo Mariani [6], Francesco Felici [1], Dario Farina [7], Deborah Falla [8], Andrea Macaluso [1], Paola Sbriccoli [1], Alessandro Del Vecchio [9]

Affiliations

[1] Department of Movement, Human and Health Sciences, University of Rome "Foro Italico", Rome, Italy

[2] Departamento de Eletrônica e Engenharia Biomédica, Faculdade de Engenharia Elétrica e de Computação, Universidade Estadual de Campinas, Brazil.

[3] Laboratório de Pesquisa em Neuroengenharia, Centro de Engenharia Biomédica, Universidade Estadual de Campinas, Brazil.

[4] Department of Biomedical Sciences, University of Padova, Padua, Italy.

[5] Physical Medicine and Rehabilitation Unit, IRCSS – Istituto Ortopedico Rizzoli, Bologna, Italy.

[6] Villa Stuart Sport Clinic – FIFA Medical Centre of Excellence, Rome, Italy

[7] Department of Bioengineering, Imperial College London, London, UK

[8] Centre of Precision Rehabilitation for Spinal Pain (CPR Spine), School of Sport, Exercise and Rehabilitation Sciences, University of Birmingham, Birmingham, UK

[9] Department of Artificial Intelligence in Biomedical Engineering, Friedrich-Alexander University Erlangen-Nürnberg, Germany

Correspondence: Stefano Nuccio (nuccio.stefano@gmail.com)

Abstract: This cross-sectional study aims to elucidate the neural mechanisms underlying the control of knee extension forces in individuals with anterior cruciate ligament reconstructions (ACLR). Eleven soccer players with ACLR and nine control players performed unilateral isometric knee extensions at 10% and 30% of their maximum voluntary force (MVF). Simultaneous recordings of high-density surface electromyography (HDEMG) and force output were conducted for each lower limb, and HDEMG data from the vastus lateralis (VL) and vastus medialis (VM) muscles were decomposed into individual motor unit spike trains. Force steadiness was estimated using the coefficient of variation of force. An intramuscular coherence analysis was adopted to estimate the common synaptic input (CSI) converging to each muscle. A factor analysis was applied to investigate the neural strategies underlying the control of synergistic motor neuron clusters, referred to as *motor unit modes*. Force steadiness was similar between lower limbs. However, motor neurons innervating the VL on the reconstructed side received a lower proportion of CSI at low-frequency bandwidths (< 5 Hz) in comparison to unaffected lower limbs ($P < 0.01$). Furthermore, the reconstructed side demonstrated a higher proportion of motor units associated with the neural input common to the synergistic muscle, as compared to unaffected lower limbs ($P < 0.01$). These findings indicate that the VL muscle of reconstructed lower limbs contribute marginally to force steadiness and that a plastic rearrangement in synergistic clusters of motor units involved in the control of knee extension forces is evident following ACLR.

New and Noteworthy: Chronic quadriceps dysfunction is common after anterior cruciate ligament reconstruction (ACLR). We investigated voluntary force control strategies by estimating common inputs to motor neurons innervating the vastii muscles. Our results showed attenuated common inputs to the vastus lateralis and plastic rearrangements in functional clusters of motor neurons modulating knee extension forces in the reconstructed limb. These findings suggest neuroplastic adjustments following ACLR that may occur to fine-tune the control of quadriceps forces.

Keywords: motor unit; ACL reconstruction; force steadiness; common synaptic input; muscle synergies.

Introduction

Restoration of quadriceps strength and function is the primary focus of rehabilitation following anterior cruciate ligament reconstruction (ACLR) (1). This is because persistent quadriceps dysfunction is common post-ACLR and is associated with severe outcomes such as an increased risk of subsequent knee injuries (2), knee osteoarthrithis (3,4), and altered biomechanics of sport-specific movements (5). The major contributing factor to quadriceps dysfunction is a debilitating neurological condition termed arthrogenic muscle inhibition (AMI), which manifests as a net involuntary inhibitory drive to the quadriceps muscle, hindering its functional recovery despite extensive post-surgical rehabilitation (6).

Evidence reported an incidence of 56% of AMI in patients at their first outpatient visit after an ACL injury (7), and 24% prevalence of quadriceps activation failure after ACLR (8). Furthermore, as a result of persistent neural impairments, ACLR patients consistently experience deficits in knee extension strength (~20%) over time, despite the completion of rehabilitation and clearance to return to sport (9-14). However, in addition to maximal strength deficits, quadriceps dysfunction can also manifest as the inability to adequately control knee extension forces during both maximal and submaximal contractions (15-21). Reduced force steadiness is shown to be unrelated to maximal strength deficits (22) and is clinically important due to its association with poor self-reported knee function (16,17) and altered running kinematics (19) post-ACLR. Therefore, a thorough understanding of the neural mechanisms behind the inability to modulate knee extension forces is a priority to improve outcomes after ACLR.

The generation and modulation of muscle forces are achieved through the activation of a set of alpha motor neurons receiving a mixture of excitatory and inhibitory signals projecting from spinal, supraspinal, and afferent pathways (23). These signals provide both independent and shared inputs to motor neurons. However, only common inputs to groups of motor neurons (i.e., common synaptic input [CSI)]) translate into the effective neural drive to muscle, which ultimately determines the volitional force produced (24-26). Coherence analysis, examining correlations in MU spike trains within and between muscles (i.e., intramuscular coherence and intermuscular coherence, respectively) in the frequency domain, is typically adopted to estimate the CSI to spinal motor neurons under various conditions, such as spinal cord injury (27) and aging (28). Additionally, the estimation of the CSI in specific frequency bandwidths is widely adopted to infer the relative contributions of different sources of the synaptic input to motor output (29). Specifically, peak coherence values within the delta (0–5 Hz), alpha (6–12 Hz) and beta (15– 35 Hz) bands are typically examined to estimate the proportion of shared inputs (i.e., CSI) linked to *a)* volitional force control (delta band), *b)* afferent inputs and tremor (alpha band), and *c)* corticospinal pathways (beta band) (30-33). Whether these inputs to the VL and VM muscles change after ACLR and their impact on both neural drive and motor output remains unknown. Furthermore, coherence analysis is typically adopted to study muscle synergies, under the assumption that a common activation signal projects to the MU pools of different muscles, thereby modulating volitional force and coordinating movements (34-36). However, a recent study by Del Vecchio and colleagues (37) extended this classic theory of muscle synergies through the assessment of synergistic clusters of MUs (rather than muscles), termed *motor unit modes*. In this novel view, common inputs are distributed to multiple groups of motor neurons, each controlling different muscles (i.e., across motor nuclei: motor neurons belonging to different muscle-related pools). This means that the central nervous system may flexibly control the activity of functional groups of motor neurons rather than entire muscle-related pools, thus reducing the dimensionality of control (37-39). Simulations and experimental data support this novel framework's ability to change the hierarchical evaluation of synergies, by assessing CSIs that are shared across MU clusters, rather than within muscle-related pools (37,38). For instance, while previous studies (35), found that the spiking activity of motor neurons activating VL and VM muscles are highly correlated (i.e., shared most of the CSI), Del Vecchio and colleagues (37) demonstrated the existence at least two independent sources of CSI that control motor neurons innervating synergistic muscles, suggesting modulation of CSIs within and between motor nuclei (37). The adoption of a factorization analysis to study the low-dimension latent component underlying the discharge rate of vastii MUs in people with ACLR would provide further evidence on the potential changes in the distribution of CSI to clusters of motor neurons underlying the synergistic control of the VL and VM muscles during sustained isometric contractions.

The primary aims of this study were to examine *a)* the CSI to the VL and VM spinal motor neurons in individuals post-ACLR and *b)* the distribution of CSI across functional clusters of motor neurons that are involved in the synergistic activation of the VL and VM muscles and in the control of steady low-intensity quadriceps forces. We hypothesized worse quadriceps force steadiness and significant changes in magnitude and distribution of common inputs controlling the activation of the VL and VM muscles of ACL reconstructed limbs.

Methods

Study Design

This cross-sectional investigation included two distinct sessions (i.e., a familiarization session and an experimental session) that were conducted 24 hours apart at the laboratory of Exercise

Physiology of the University of Roma "Foro Italico". During these sessions, participants performed low-intensity sustained isometric contractions at 10% and 30% of maximal voluntary force (MVF), during which knee extension forces and high-density surface electromyographic (HDEMG) signals from the VL and VM muscles were concurrently recorded. The report followed the recommendations of the *Strengthening the Reporting of Observational Studies in Epidemiology* (STROBE) checklist.

Participants

Eleven male soccer players with ACLR (24.8 ± 3.2 years) and nine male healthy soccer players (25.7 ± 2.5 years), with similar anthropometric characteristics and physical activity levels (**Table 1**), were recruited from clinic rosters and university classes. All patients with ACLR were operated by the same orthopedic surgeon within thirty days after surgery and followed the same rehabilitation process. History of previous knee injury or surgery, presence of neuromuscular disorders or anterior knee pain were adopted as exclusion criteria. Ethical approval for all procedures was obtained from the Internal Review Board of the University of Rome "Foro Italico" (n.2018/07), and the study adhered to the standards outlined in the *Declaration of Helsinki*. Written informed consent was obtained from all participants before their first experimental session.

Experimental Procedures

The neuromuscular assessment was conducted on both lower limbs of each experimental group. A KinCom dynamometer (KinCom, Denver, CO, USA) was set to measure unilateral knee extension forces. Participants were comfortably seated and fastened to the device using straps and apposite cuffs, to minimize lower limb movements. The knee and hip joints were set at a flexion angle of 45° (full knee extension = 0°) and 100° (180° = anatomical position), respectively, and the rotational axis of the dynamometer was aligned with the medial femoral condyle. Preceding the assessments, skin preparation was undertaken, involving shaving and cleansing with 70% ethanol solution. Two bi-dimensional grids of 64 golden-coated electrodes (model ELSCH064NM2; 8 mm of inter-electrode space; OT Bioelettronica, Turin, Italy) were positioned on the skin surface overlying the VL and VM muscles, adhering to the standards proposed by Barbero and colleagues (40). HDEMG grids were attached to the skin using bi-adhesive foam layers (SpesMedica, Battipaglia, Italy). Reference and ground electrodes were affixed on the patella, medial malleolus, and contralateral wrist. Force and monopolar HDEMG signals were simultaneously recorded with a multichannel amplifier (EMG-Quattrocento; resolution of 16 bits; OT Bioelettronica, Turin, Italy), sampled at 2048 Hz and collected using the software OTBioLab (OT Bioelettronica, Turin, Italy). To determine the maximum voluntary force (MVF) and set submaximal task levels, participants first performed three maximal isometric contractions, each separated by 60-second of rest. During these trials participants received strong verbal support to "push as hard as possible" and overcome the peak reached in previous maximal contractions. Afterwards, participants performed two ~ 60s steady force-matching contractions at force levels corresponding to 10% and 30% of MVF, with a 60-second of rest between them. Among the two isometric contractions at each force target (i.e., 10 and 30% MVF), only the one demonstrating the highest accuracy in replicating the prescribed force trajectory, was selected for the analysis for each participant (41). Real-time visual feedback was provided to participants, with both the actual force output and the anticipated trajectory, with a constant visual gain.

Data processing and analysis

Knee extension force

The force signals were converted to Newtons (N), adjusted by subtracting the gravitational signal offset, normalized relative to MVF and low-pass filtered using a zero-lag Butterworth filter of 4th order, with a cut-off frequency of 15Hz. The coefficient of variation of force (Force$_{CoV}$) was then computed to determine force fluctuations and steadiness (42).

MU decomposition and properties

The decomposition procedures adopted in this study have been comprehensively detailed in prior studies (12). Briefly, monopolar HDEMG signals were bandpass filtered between 20 and 500 Hz with a second-order Butterworth filter and decomposed into individual MU discharge times using a valid blind source separation method (43) implemented in a MATLAB (R2020a; The MathWorks, Natick, MA) tool (DEMUSE; The University of Maribor, Slovenia). The identified discharge times of individual MUs were initially converted into binary spike-trains. Subsequently, the spiking activity of all identified MUs was visually inspected by an expert operator for further analysis. The pulse-to-noise ratio (PNR) was used to evaluate the accuracy of the decomposition method and MUs exhibiting poor signal quality (i.e., PNR values ≤ 30 dB denoting decomposition accuracy ≤ 90%) and/or those with inter-spike intervals exceeding 2 seconds were excluded from analysis (44). Each valid MU spike train was then visually inspected and manually edited following published guidelines (45). To account for potential task-related adjustments in motor unit discharge rate (MU DR), all neuromuscular analyses were carried out on the central 30-second segment of steady contractions. Steady contractions with fewer than four confirmed MUs were discarded. MU DR and the coefficient of variation for the inter-spike Interval (CovISI) were estimated during the 30-second segment of each steady contraction.

Intramuscular Coherence

To estimate the common input that is shared among motor neurons innervating the same muscle (i.e., VL or VM) an intramuscular coherence analysis (IMC; **Figure 2**) was performed on two equally-sized cumulative spike trains (i.e., index of the neural drive to the muscle; CSTs). Specifically, CSTs were cross-correlated for increasing groups of MUs (e.g., six identified MUs were pooled into two groups containing up to three MUs each) using a Welsh periodogram with non-overlapping 1-second Hanning windows. The average of 100 random permutations of the identified MUs was extracted for subsequent analysis. Coherence profiles were estimated across the full-frequency bandwidth (29) and peaks within delta (1–5 Hz), alpha (6 –12 Hz) and beta (15-30 Hz) bands were identified and analyzed. The average coherence in the frequency range of 100-250 Hz was set as the *bias* level and, therefore, subtracted from the analyses of coherence profiles (46). The proportion of common synaptic input (PCI) relative to the total input received by motor neurons was estimated for each participant as rate of increase in low-frequency coherence when increasing the number of identified MUs (47,48). The PCI represents the fraction of the synaptic input that is shared between motor neurons which, as a result, do not reflect independent synaptic components.

Factor analysis

The factor analysis followed the procedures described by Del Vecchio and colleagues (37). MU discharge times were smoothed using a 400 ms Hann window. To remove any *a priori* assumption on muscle-specificity, the MUs of the VL and VM muscles were pooled together, and two main factors were identified, representing low-dimensional latent components explaining most of the variance of the pooled motor unit discharge rate. Subsequently, these factors were correlated with the neural drive (i.e., the averaged instantaneous discharge rate of MUs) of each muscle. This correlation aimed to redefine the factors as the VL Module and VM Module, given the initial absence of a clear association between the first and second factor and the individual muscles. We then defined arbitrary and conservative centroids ([0.65 1.00], [0.40 0.40], [1.00 0.65]) to classify the entire MU population into the VL, mixed or VM clusters, based on the bivariate correlation between modules and the smoothed discharge rate of each MU. Then, we redefined these groups for each muscle as “Self”, “Mixed” and “Other” clusters, representing the proportion of MUs associated with a) the dominant muscle-specific *motor unit mode* (i.e., Self), denoting MUs predominantly correlated with the factor specific to the muscle in which they reside (e.g., VL Module for the VL muscle), b) the *motor unit mode* correlated with the factors of both muscles (i.e., Mixed) and c) the *motor unit mode* associated with the synergistic muscle (i.e., Other), representing MUs identified in one muscle that are primarily correlated with the factor of the other muscle (e.g., VM Module for the VL muscle).

For instance, when considering all the MUs identified from the decomposition of the HD-EMG signal from the VL muscle, the "Self" cluster indicated the proportion of MUs that were correlated with the VL module. Conversely, the "Other" cluster indicated the proportion of MUs identified in the VL that were correlated with the VM Module. The "Mixed" cluster represented the proportion of MUs that were correlated with both VL and VM Modules, indicating synergistic muscle activations. In this regard, Del Vecchio and colleagues (37) conducted a computer simulation performed on 480 integrate-and-fire neurons, that demonstrated the robustness and validity of the factorization analysis approach for the identification of distinct *motor unit modes*.

Statistical Analysis

A Shapiro-Wilk test was used to confirm the assumption of normal data distribution for each of the dependent variable under investigation. Separate linear mixed models were then adopted to test interlimb differences (GAMLj pack: General Analyses for the Linear Model in Jamovi). To account for the variability in the number of the identified MUs for each participant, avoid pseudo-replication, and control for the non-independence of observations from the same individuals (i.e., two lower limbs tested), participants were included in mixed models as random intercept. To investigate differences in motor unit properties, separate mixed models were run for MU DR and CovISI (i.e., dependent variables), including side (Reconstructed, Contralateral, Dominant and Non Dominant), muscle (VL and VM), and target force (10%MVF and 30%MVF) as fixed factors. Differences in force steadiness (CoVForce) and coherence (PCI, Delta, Alpha, and Beta coherence) were investigated using separate linear models. Additionally, the output of the factor analysis (i.e., proportion of MUs within the Self, Mixed and Other clusters) was examined using a linear model that was designed with side, muscle, target force and cluster as fixed factors. To account for the baseline differences in MVF of the ACLR group, the level of MVF displayed by participants was included as a covariate in each of these models. The significance of the fixed effect was assessed by an F-test using Satterthwaite's method to approximate the degrees of freedom. A Gamma distribution and a Log link function were used for modeling non-normal positively-skewed data. A Bonferroni-Holm correction was applied when needed to account for multiple comparisons during post-hoc analysis. All data are reported as mean ± standard deviation (SD) unless otherwise specified. The significance level was set at $P < 0.05$.

Results

Demographics, Force and MU properties

Participants' descriptive and clinical characteristics, and maximal knee extension force levels are reported in **Table 1**. No significant side-by-group interaction were found for the $Force_{CoV}$ at both 10% (Reconstructed: 2.48 ± 0.64 %; Contralateral: 2.09 ± 0.40 %; Dominant: 2.57 ± 0.83 %; Non Dominant: 2.20 ± 0.79 %; $P > 0.05$) and 30% (Reconstructed: 2.37 ± 0.77 %; Contralateral: 2.53 ± 0.98 %; Dominant: 1.84 ± 0.47 %; Non Dominant: 2.03 ± 0.55 %; $P > 0.05$) of the MVF, indicating neither within (i.e., across lower limbs) nor between (i.e., across groups) differences in force steadiness. When considering each lower limb (i.e., Reconstructed, Contralateral, Dominant and Non Dominant), group (i.e., ACLR and CONTROL) and submaximal contraction (i.e., 10% and 30% MVF), a total of 694 and 530 unique MUs were identified through the decomposition analysis from the VL and VM muscles, respectively, with an average of 9.4 ± 3.7 and 7.6 ± 3.4 MUs per participant. There were no significant between-side differences in MU DR and CovISI (**Figure 3**; $P > 0.05$).

IMC

Figure 4 shows lower-limb specific profiles of IMC for both muscles and contraction levels (panels **A-D**) and band-specific values obtained from each participant for the Delta (panel **E**), Alpha (panel **F**) and beta bands (panel **G**). A significant effect of side ($X^2 = 11.4$, $P = 0.01$), task ($X^2 = 4.2$, $P = 0.041$), muscle ($X^2 = 4.5$, $P = 0.033$) and side*muscle interaction ($X^2 = 9.3$, $P = 0.025$) was found for the Delta band. Post-hoc analyses showed significantly lower Delta band magnitudes for the VL in the Reconstructed side (10% MVF: 0.08 ± 0.04; 30% MVF: 0.07 ± 0.04) with respect to the Contralateral side (30% MVF: 0.22 ± 0.16; $P < 0.001$) and to both the Dominant (10% MVF: 0.18 ± 0.11; $P = 0.024$; 30% MVF: 0.24 ± 0.12; $P < 0.001$) and Non Dominant lower limbs (10% MVF: 0.18 ± 0.018; $P = 0.024$; 30% MVF: *vs* 0.22 ± 0.12; $P < 0.001$) of the Control group (**Figure 3E**). Coherence within Alpha and Beta bands were similar across sides, muscles, and contraction levels ($P > 0.05$, **Figure 4F-G**).

The analysis of PCI revealed a significant main effect of side ($X^2 = 11.3$, $P = 0.01$) and muscle ($X^2 = 5.3$, $P = 0.021$) and a significant side*muscle interaction ($X^2 = 10.3$, $P = 0.016$). Post-hoc analysis revealed that **t**he PCI received by the VL of the reconstructed side (10% MVF: 0.269 ± 0.117; 30%

MVF: 0.302 ± 0.219) was lower when compared to the Dominant (10% MVF: 0.672 ± 0.391; P = 0.001; 30% MVF: 0.873 ± 0.426; P = 0.002), Non Dominant (10% MVF: 0.660 ± 0.308; P = 0.002; 30% MVF: 0.762 ± 0.436; P = 0.009) and Contralateral sides (30% MVF: 0.727 ± 0.523; P = 0.011) (**Figure 5-6**).

Factor Analysis

The generalized linear model adopted to study the between-side difference in MU cluster proportions revealed a significant side*cluster interaction ($X^2 = 19.38$, P = 0.004). Post-hoc analysis revealed that, overall, the proportion of MUs grouped in the Other cluster was higher for the Reconstructed side (19.2% ± 14.4%) when compared to the Contralateral (13.1% ± 10.8%; P = 0.02), Dominant (11.6% ± 10.4%; P< 0.01) and Non Dominant (12% ± 9.7%; P< 0.01) sides (**Figure 7E**). No significant differences (P > 0.05) were found for the Self (**Figure 7C**) and Mixed clusters (**Figure 7D**).

Discussion

We examined the intramuscular coherence and the synergistic activation of the VL and VM muscles to determine the neural strategies underlying force control in individuals with ACLR. Force steadiness and motor unit firing patterns were similar between the reconstructed and unaffected limbs, but motor neurons innervating the VL of the reconstructed side received a lower proportion of common synaptic input when compared to the contralateral side and healthy lower limbs. Remarkably, the factor analysis confirmed the presence of more than one common input received by the pool of motor neurons and revealed, for the first time, plastic rearrangements in functional clusters of MUs following ACLR, as indicated by the significantly higher proportion of MUs that were associated with the *motor unit mode* of the synergistic muscle ("Other" cluster) in the Reconstructed side when compared to uninjured lower limbs. These findings suggest that motor neurons modulating the activity of the VL in the reconstructed limb received an increased proportion of independent over common synaptic inputs and that the contribution of the VL to force steadiness during low-intensity force-matching tasks is marginal. Additionally, the differences found in the synergistic control of functional clusters of MUs support the hypothesis that the central nervous system can flexibly recruit motor neurons of different pools and that the neural strategy adopted to control the simultaneous activation of the VL and VM can change in response to ACLR.

The recovery of quadriceps function is the primary focus of rehabilitation following ACLR. However, despite full efforts to achieve this goal, there is consistent evidence of persistent quadriceps dysfunction and voluntary activation deficits several months post-surgery (9-11).

Further, previous evidence demonstrated short- and long-term quadriceps force control impairments, consisting of large force fluctuations and poor force-matching accuracy during both maximal and submaximal knee extension tasks (15-22). Not surprisingly, our sample of ACLR patients showed significant deficits in MVF but, in contrast to our hypothesis, we found similar force steadiness and motor unit output (i.e., unaltered MU DR and CovISI) across lower limbs and groups.

These divergences in motor output deficits (i.e., reduced quadriceps strength but similar force control) denote that these indexes provide distinct information and are not interdependent. This assumption is supported by Johnson et al. (22) who have recently documented no significant correlations between torque peak and variability during maximal knee extensions performed by individuals with ACLR. Our findings suggest optimal control of knee extension forces of our sample of ACLR individuals and agree with Sherman and colleagues (21) who documented greater root mean square error but similar coefficient of variation of force in individuals with ACLR compared to matched controls, during force-tracing tasks at 50% of MVF. However, it should be noted that force steadiness ultimately depends on the ensemble properties of all the muscles involved (30) and that it can be modulated by factors such as muscle coactivation (15-18), motor unit contractile properties (30) and recruitment strategies (49) which, collectively, may have contributed to force control in our sample of athletes with ACLR.

MU DR and CovISI were similar between sides and groups. Interspike interval variability is known to increase in response to highly fluctuating excitatory and inhibitory synaptic inputs to motor neurons and to influence force steadiness (49). The unchanged pattern of CovISI may thus reflect the absence of random background activity in synaptic inputs (i.e., synaptic noise) following ACL surgery (23,30). On the other hand, the unaltered MU DR was accompanied by reduced Delta coherence and PCI in the VL of the Reconstructed side with respect to both the contralateral side and control lower limbs. The common input to spinal motor neurons within the low-frequency bandwidth (i.e., <5 Hz, Delta) is known to mirror the effective neural drive to the muscle, with a gain that is regulated by neuromodulation (25,50). Together with the similar motor unit output (i.e., similar MU DR), these findings on CSI and PCI could suggest that, compared to uninjured limbs, *a)* the activity of the VL of the reconstructed side is dominated by a higher proportion of independent synaptic inputs (28) which have little to no influence on the neural drive to muscle, *b)* the lower contribution of the VL muscle to force steadiness is potentially compensated by the VM or other muscles involved in knee extension tasks (30), and *c)* there could be an effect of neuromodulation on the observed motor unit output. A decreased low-frequency coherence between MU firings may result from an AMI-related increase in pre-synaptic inhibitory inputs to motor neurons from cortical pathways (6) affecting CSIs that are effectively transmitted to spinal motor neurons. Additionally, although not directly assessed in the current study, changes in muscle unit properties of the VL could have had an impact on these findings (51).

Proportions of CSI within the Alpha and Beta coherence bands were similar between limbs. Increased neural oscillation in the alpha band are indicative of physiologic tremor which ultimately interfere with accurate force production (29-33). Such an involuntary common synaptic noise is determined by changes in afferent inputs, which are typically impaired after ACL injury and reconstruction due to deafferentation, increased joint laxity and gamma-loop dysfunction mechanisms (6). Our finding of unaltered alpha oscillations agrees with recent studies and reviews demonstrating a full recovery or improvement of spinal-reflexive excitability several months post-surgery (9,10,52). Nonetheless, interestingly, some reconstructed limbs in our sample of ACLR participants showed a peak within 8-10 Hz (e.g., the representative coherence profile in **Figure 2B**), suggesting that, potentially, some individuals may display residual alterations in afferent inputs, leading to long-term impairment in sensorimotor integration and motor output post-ACLR. However, future studies are needed to confirm this observation. Oscillations in the higher frequency bandwidths (i.e., 15-35 Hz) are reflective of corticospinal input transmission and are hypothesized to play a role in both neurological disorders and motor control (53,54). However, due to the low-pass filtering properties of muscles, beta inputs are supposed to have a marginal influence on voluntary force production (24,25). Zicher and colleagues (32) reinforced this conclusion, demonstrating that small changes in muscle force can be only determined by bursts of beta activity which, however, due to their sporadic and irregular nature, potentially have a negligible impact the voluntary control of force. Our findings of similar coherence in this high-frequency bandwidths agree with this recent evidence and indicate that beta oscillations do not contribute to common AMI-related cortical impairments underlying quadriceps dysfunction following ACLR (6).

To study the neural connectivity between the VL and VM we adopted a factor analysis (37) which consisted in the assessment of the strength of correlation between the discharge properties of all MUs recruited during the sustained isometric knee extension tasks, without any *a priori* muscle-related constraint. In agreement with recent evidence (37,38,55), the spiking activities of the VL and VM were modulated by two main modules with CSI spread across functional clusters of MUs.

Functionally, the concerted activation of VL and VM muscles provides knee extension forces, patellofemoral stabilization, and mitigation of internal joint stresses (38,56). Therefore, the presence of more than one CSI controlling the activity of functional clusters of motor neurons suggests a more flexible and independent control of these two important functions with respect to the classic view of muscle-specific pool of MUs. Interestingly, the reconstructed side showed higher proportions of MUs that were correlated with the activity of the synergistic muscle ("Other" cluster) when compared to uninjured lower limbs. This finding suggests that clusters of motor neurons are not rigid and that they can change plastically as a result of neural adaptations to quadriceps dysfunction following ACLR.

Limitations

The relatively small number of participants represents a potential limitation of this study. Given the documented inter-individual variability in the neural control of the VL and VM (57), further investigations, including larger samples of ACLR individuals, are needed to reinforce the generalizability of our findings. Furthermore, although the identification of specific clusters was not an aim of the current study, it should be considered that *motor unit modes* were identified by arbitrarily selecting boundaries based on correlations with specific centroids (37). It should be also recognized that few uncontrolled factors such as quadriceps morphological changes (51), hamstring coactivation (15,18) and the contribution of other muscles to the control of knee extension forces may have contributed to the force steadiness observed in the ACLR group. Additionally, future studies should be designed to explore motor unit synergies in individuals with ACLR during force-matching tasks reaching high force levels. Lastly, longitudinal investigations are encouraged to infer causal relationships and provide solid insights into both the neuroplastic changes following ACLR and the relation between quadriceps activation failure and changes in proportions of common synaptic inputs.

Conclusions

In conclusion, when compared to uninjured lower limbs, motor neurons innervating the VL of reconstructed limbs received attenuated common inputs in the low-frequency bandwidth, suggesting a reduced contribution to volitional force. Furthermore, the reconstructed side had an increased proportion of motor neurons whose discharge behavior was not related to the muscle they innervated, but rather to the synergistic muscle, suggesting potential ACLR-related adjustments in the way the central nervous system controls the activity of functional clusters of motor neurons innervating the quadriceps muscle. This study provides new insights into the strategies adopted to control knee extension forces following ACLR. However, further research is needed to understand the clinical implications of these findings.

Data Availability Statement

The data that support the findings of this study are available from the corresponding author upon reasonable request.

Acknowledgments

The authors would like to acknowledge all the volunteers who participate with enthusiasm and commitment to the study and BioRender.com for providing the tools to create the scientific illustrations used in this publication.

Grants

This work was partly supported by the European Research Council (ERC) Starting Grant project GRASPAGAIN under grant 101118089 and by the German Ministry for Education and Research (BMBF) through the project MYOREHAB under Grant 01DN2300.

Disclosures

None of the authors has any conflicts of interests.

Author Contribution

SN, PS, AM and ADV conceived and designed the work. SN, CMG, AC and ADV analyzed the data. SN performed experiments, drafted the manuscript, and plotted the figures. All authors revised it critically for important intellectual content, approved the final version of the manuscript and agree to be accountable for all aspects of the work. All persons designated as authors qualify for authorship, and all those who qualify for authorship are listed.

References

1. **Buckthorpe M, La Rosa G, Della Villa F.** Restoring Knee Extensor Strength After Anterior Cruciate Ligament Reconstruction: a Clinical Commentary. *Intern J Sports Phys Ther*, 14: 159-172, 2019. https://doi.org/10.26603/ijspt20190159
2. **Grindem H, Snyder-Mackler L, Moksnes H, Engebretsen L, Risberg MA.** Simple decision rules can reduce reinjury risk by 84% after ACL reconstruction: The Delaware-Oslo ACL cohort study. *Br J Sports Med* 50: 804–808, 2016. https://doi.org/10.1136/bjsports-2016-096031
3. **Pietrosimone B, Pfeiffer SJ, Harkey MS, Wallace K, Hunt C, Blackburn JT, Schmitz R, David Lalush D, Nissman D, Spang JT.** Quadriceps weakness associates with greater T1ρ relaxation time in the medial femoral articular cartilage 6 months following anterior cruciate ligament reconstruction. *Knee Surg Sports Traumatol Arthrosc* 27: 2632-2642, 2019. https://doi.org/10.1007/s00167-018-5290-y

4. **Bodkin SG, Werner BC, Slater LV, Hart JM.** Post-traumatic osteoarthritis diagnosed within 5 years following ACL reconstruction. *Knee Surg Sports Traumatol Arthrosc*, 28: 790-796, 2020. https://doi.org/10.1007/s00167-019-05461-y
5. **Kyritsis P, Bahr R, Landreau P, Miladi R, Witvrouw E.** Likelihood of ACL graft rupture: not meeting six clinical discharge criteria before return to sport is associated with a four times greater risk of rupture. *Br J Sports Med* 50: 946-951, 2016. https://doi.org/10.1136/bjsports-2015-095908
6. **Lepley AS, Lepley LK.** Mechanisms of Arthrogenic Muscle Inhibition. *J Sport Rehab* 31: 707–716, 2022. https://doi.org/10.1123/jsr.2020-0479
7. **Sonnery-Cottet B, Hopper GP, Gousopoulos L, Pioger C, Vieira TD, Thaunat M, Fayard J-M, Freychet B, Cavaignac E, Saithna A.** Incidence of and Risk Factors for Arthrogenic Muscle Inhibition in Acute Anterior Cruciate Ligament Injuries: A Cross-Sectional Study and Analysis of Associated Factors From the SANTI Study Group. *Am J Sports Med* 52: 60-68, 2024. https://doi.org/10.1177/03635465231209987
8. **Hurt JM, Pietrosimone B, Hertel J, Ingersoll CD.** Quadriceps Activation Following Knee Injuries: A Systematic Review. *J Athl Train* 45: 87-97, 2010. https://doi.org/10.4085/1062-6050-45.1.87
9. **Lepley AS, Gribble PA, Thomas AC, Tevald MA, Sohn DH, Pietrosimone BG.** Quadriceps neural alterations in anterior cruciate ligament reconstructed patients: A 6-month longitudinal investigation. *Scand J Med Sci Sports* 25: 828-39, 2015 https://doi.org/10.1111/sms.12435
10. **Tayfur B, Charuphongsa C, Morrissey D, Miller SC.** Neuromuscular Function of the Knee Joint Following Knee Injuries: Does It Ever Get Back to Normal? A Systematic Review with Meta-Analyses. *Sports Med* 51, 321-338, 2021. https://doi.org/10.1007/s40279-020-01386-6
11. **Lisee C, Lepley AS, Birchmeier T, O'Hagan K, Kuenze C.** Quadriceps Strength and Volitional Activation After Anterior Cruciate Ligament Reconstruction: A Systematic Review and Meta-analysis. *Sports Health* 11:163-179, 2019. https://doi.org/10.1177/1941738118822739
12. **Nuccio S, Del Vecchio A, Casolo A, Labanca L, Rocchi JE, Felici F, Macaluso A, Mariani PP, Falla D, Farina D, Sbriccoli P.** Deficit in knee extension strength following anterior cruciate ligament reconstruction is explained by a reduced neural drive to the vasti muscles. *J Physiol* 599: 5103–5120, 2021. https://doi.org/10.1113/JP282014
13. **Nuccio S, Del Vecchio A, Casolo A, Labanca L, Rocchi JE, Felici F, Macaluso A, Mariani PP, Falla D, Farina D, Sbriccoli P.** Muscle fiber conduction velocity in the vastus lateralis and medialis muscles of soccer players after ACL reconstruction. *Scand J Med Sci Sports* 30: 1976-1984, 2020. https://doi.org/10.1111/sms.13748

14. **Sherman DA, Rush J, Stock MS, D. Ingersoll CE. Norte G.** Neural drive and motor unit characteristics after anterior cruciate ligament reconstruction: implications for quadriceps weakness. *PeerJ* 11: e16261, 2023.https://doi.org/10.7717/peerj.16261
15. **Telianidis S, Perraton L, Clark RA, Pua Y-H, Fortin K, Bryant AD.** Diminished sub-maximal quadriceps force control in anterior cruciate ligament reconstructed patients is related to quadriceps and hamstring muscle dyskinesia. *J Electromyogr Kinesiol* 24: 513-519, 2014. https://doi.org/10.1016/j.jelekin.2014.04.014
16. **Goetschius J, Hart JM.** Knee-Extension Torque Variability and Subjective Knee Function in Patients with a History of Anterior Cruciate Ligament Reconstruction. *J Athl Train* 51: 22-7, 2016. https://doi.org/10.4085/1062-6050-51.1.12
17. **Perraton L, Clark R, Crossley K, Pua YH, Whitehead T, Morris H, Telianidis S, Bryant A.** Impaired voluntary quadriceps force control following anterior cruciate ligament reconstruction: relationship with knee function. *Knee Surg Sports Traumatol Arthrosc* 25: 1424-1431, 2016. https://doi.org/10.1007/s00167-015-3937-5
18. **Rice D, Lewis G, McNair P.** Impaired Regulation of Submaximal Force after ACL Reconstruction: Role of Muscle Spindles. *Int J Sports Med* 42: 550-558, 2021. https://doi.org/10.1055/a-1292-4461
19. **Spencer A, Davis K, Jacobs C, Johnson D, Ireland ML, Noehren B.** Decreased quadriceps force steadiness following anterior cruciate ligament reconstruction is associated with altered running kinematics. *Clin Biomech (Bristol, Avon)* 72:58-62, 2020. https://doi.org/10.1016/j.clinbiomech.2019.11.021
20. **Ward SH, Perraton L, Bennell K, Pietrosimone B, Bryant AL.** Deficits in Quadriceps Force Control After Anterior Cruciate Ligament Injury: Potential Central Mechanisms. *J Athl Train* 54: 505-512, 2019. http://https//doi.org/10.4085/1062-6050-414-17
21. **Sherman DA, Baumeister J, Stock MS, Murray AM, Bazett-Jones DM, Norte GE.** Weaker Quadriceps Corticomuscular Coherence in Individuals Following ACL Reconstruction during Force Tracing. *Med Sci Sports Exer*. 55: 625-632, 2022. https://doi.org/10.1249/MSS.0000000000003080
22. **Johnson AK, Rodriguez KM, Lepley AS, Palmieri-Smith RM.** Quadriceps torque complexity before and after anterior cruciate ligament reconstruction. *J Sci Med Sport* 26: 533-538, 2023. https://doi.org/10.1016/j.jsams.2023.09.009
23. **Heckman CJ, Enoka RM.** Motor Unit. *Compr Physiol*, 2: 2629-2682, 2012. https://doi.org/10.1002/cphy.c100087
24. **Farina D, Negro F.** Common Synaptic Input to Motor Neurons, Motor Unit Synchronization,

and Force Control. *Exerc Sport Sci Rev* 43: 23-33, 2015. https://doi.org/10.1249/JES.0000000000000032

25. **Farina D, Negro F, Muceli S, Enoka RM.** Principles of Motor Unit Physiology Evolve With Advances in Technology. *Physiology (Bethesda)* 31: 83-94, 2016. https://doi.org/10.1152/physiol.00040.2015.
26. **Thompson CK, Negro F, Johnson MD, Holmes MR, McPherson LM, Powers RK, Farina D, Heckman CJ.** Robust and accurate decoding of motoneuron behaviour and prediction of the resulting force output. *J Physiol* 596: 2643-2659, 2018. https://doi.org/10.1113/JP276153
27. **Gogeascoechea A, Kuck A, Van Asseldonk E, Negro F, Buitenweg JR, Yavuz US, Sartori M.** Interfacing With Alpha Motor Neurons in Spinal Cord Injury Patients Receiving Trans-spinal Electrical Stimulation. *Front Neurol*. 11: 493, 2020. https://doi.org/10.3389/fneur.2020.00493
28. **Castronovo AM, Mrachacz-Kersting N, Stevenson AJT, Holobar A, Enoka RM, Farina D.** Decrease in force steadiness with aging is associated with increased power of the common but not independent input to motor neurons. *J Neurophysiol*, 120: 1616–1624, 2018. https://doi.org/10.1152/jn.00093.2018
29. **Farina D, Castronovo AM, Vujaklija I, Sturma A, Salminger S, Hofer C, Aszmann O.** Common synaptic input to motor neurons and neural drive to targeted reinnervated muscles. *J Neurosci* 37: 11285-11292, 2017. https://doi.org/10.1523/JNEUROSCI.1179-17.2017
30. **Enoka RM, Farina D.** Force steadiness: From motor units to voluntary actions. *Physiol* 36: 114-130, 2021. https://doi.org/10.1152/physiol.00027.2020
31. **Lecce E, Nuccio S, Del Vecchio A, Conti A, Nicolò A, Sacchetti M, Felici F, Bazzucchi I.** Sensorimotor integration is affected by acute whole-body vibration: a coherence study. *Front Physiol* 14:1266085, 2023. https://doi.org/10.3389/fphys.2023.1266085
32. **Zicher B, Ibáñez J, Farina D.** Beta inputs to motor neurons do not directly contribute to volitional force modulation. *J Physiol* 601: 3173-3185, 2023 https://doi.org/10.1113/JP283398
33. **Cabral HV, Inglis JG, Cudicio A, Cogliati M, Orizio C, Yavuz US, Negro F.** Muscle contractile properties directly influence shared synaptic inputs to spinal motor neurons. *J Physiol* Epub ahead of print, 2024 https://doi.org/10.1113/JP286078
34. **Bizzi E, Cheung VC.** The neural origin of muscle synergies. *Front Comput Neurosci* 7: 51, 2013. https://doi.org/10.3389/fncom.2013.00051
35. **Laine CM, Martinez-Valdes E, Falla D, Mayer F, Farina D.** Motor neuron pools of synergistic thigh muscles share most of their synaptic input. *J Neurosci* 35: 12207–12216, 2015. https://doi.org/10.1523/JNEUROSCI.0240-15.2015

36. **Latash ML**. Understanding and Synergy: A Single Concept at Different Levels of Analysis? *Front Syst Neurosci* 15: 735406, 2021. https://doi.org/10.3389/fnsys.2021.735406

37. **Del Vecchio A, Marconi Germer C, Kinfe TM, Nuccio S, Hug F, Eskofier B, Farina D, Enoka RM.** The Forces Generated by Agonist Muscles during Isometric Contractions Arise from Motor Unit Synergies. *J Neurosci* 43: 2860-2873. https://doi.org/10.1523/JNEUROSCI.1265-22.2023

38. **Hug F, Avrillon S, Ibáñez J, Farina D.** Common synaptic input, synergies, and size principle: Control of spinal motor neurons for movement generation. *J Physiol* 601: 11-20, 2022. https://doi.org/10.1113/JP283698

39. **Madarshahian S, Letizi J, Latash ML.** Synergic control of a single muscle: The example of flexor digitorum superficialis. J Physiol 599:1261-1279, 2021. https://doi.org/10.1113/jp280555

40. **Barbero M, Merletti R, Rainoldi A.** *Atlas of Muscle Innervation Zones*. Springer Milan, 2012.

41. **Casolo A, Maeo S, Balshaw TG, Lanza MB, Martin NRW, Nuccio S, Moro T, Paoli A, Felici F, Maffulli N, Eskofier B, Kinfe TM, Folland JP, Farina D, Del Vecchio AD.** Non-invasive estimation of muscle fibre size from high-density electromyography. *J Physiol*, 601: 1831-1850, 2023. https://doi.org/10.1113/JP284170

42. **Feeney DF, Mani D, Enoka RM.** Variability in common synaptic input to motor neurons modulates both force steadiness and pegboard time in young and older adults. *J Physiol* 596: 3793-3806, 2018. https://doi.org/10.1113/jp275658

43. **Holobar, Aleš, & Zazula, D.** Multichannel blind source separation using convolution Kernel compensation. *IEEE Trans Signal Process* 55: 4487-4496, 2007. https://doi.org/10.1109/TSP.2007.896108

44. **Lecce E, Nuccio S, Del Vecchio A, Conti A, Nicolò A, Sacchetti M, Felici F, Bazzucchi I.** The acute effects of whole-body vibration on motor unit recruitment and discharge properties. *Front Physiol* 14: 1124242, 2023. https://doi.org/10.3389/fphys.2023.1124242

45. **Del Vecchio A, Holobar A, Falla D, Felici F, Enoka RM, Farina D.** Tutorial: Analysis of motor unit discharge characteristics from high-density surface EMG signals. *J Electromyogr Kinesiol* 53: 102426, 2020. https://doi.org/10.1016/j.jelekin.2020.102426

46. **Del Vecchio A, Germer CM, Elias LA, Fu Q, Fine J, Santello M, Farina D.** The human central nervous system transmits common synaptic inputs to distinct motor neuron pools during non-synergistic digit actions. *J Physiol* 597: 5935-5948, 2019. https://doi.org/10.1113/JP278623

47. **Negro F, Yavuz UŞ Farina D.** The human motor neuron pools receive a dominant slow-varying common synaptic input. *J Physiol* 594: 5491-5505, 2016. https://doi.org/10.1113/JP271748

48. **Hug F, Del Vecchio A, Avrillon S, Farina D, Tucker K.** Muscles from the same muscle group do not necessarily share common drive: evidence from the human triceps surae. *J Appl Physiol* 130: 342–354, 2021. https://doi.org/10.1152/japplphysiol.00635.2020
49. **Dideriksen JL, Negro F, Enoka RM, Farina D.** Motor unit recruitment strategies and muscle properties determine the influence of synaptic noise on force steadiness. *J Neurophysiol* 107: 3357-3369, 2012. https://doi.org/10.1152/jn.00938.2011
50. **Farina D, Negro F, Dideriksen JL.** The effective neural drive to muscles is the common synaptic input to motor neurons. *J Physiol* 592: 3427-3441, 2014. https://doi.org/10.1113/jphysiol.2014.273581
51. **Nohren B, Andersen A, Hardy P Johnson, DL, Ireland ML, Thompson KL, Damon B**. Cellular and Morphological Alterations in the Vastus Lateralis Muscle as the Result of ACL Injury and Reconstruction. *J Bone Joint Surg* 98: 1541-1547, 2016 https://doi.org/10.2106/JBJS.16.00035
52. **Harkey MS, Luc-Harkey BA, Lepley AS, Grindstaff TL, Gribble P, Blackburn JT, Spang JT, Pietrosimone B.** Persistent Muscle Inhibition after Anterior Cruciate Ligament Reconstruction: Role of Reflex Excitability. *Med Sci Sports Exerc* 48: 2370-2377, 2016. https://doi.org/10.1249/MSS.0000000000001046
53. **Proudfoot M, van Ede F, Quinn A, Colclough GL, Wuu J, Talbot K, Benatar M, Woolrich MW, Nobre AC, Turner MR.** Impaired corticomuscular and interhemispheric cortical beta oscillation coupling in amyotrophic lateral sclerosis. *Clin Neurophysiol* 129: 1479-1489, 2018. https://doi.org/10.1016/j.clinph.2018.03.019
54. **Watanabe RN, Kohn AF.** Fast Oscillatory Commands from the Motor Cortex Can Be Decoded by the Spinal Cord for Force Control. *J Neurosci* 35: 13687-97, 2015 https://doi.org/10.1523/JNEUROSCI.1950-15.2015
55. **Hug F, Avrillon S, Sarcher A, Del Vecchio A, Farina D.** Correlation networks of spinal motor neurons that innervate lower limb muscles during a multi-joint isometric task. *J Physiol* 601: 3201-3219, 2023. https://doi.org/10.1113/JP283040
56. **Alessandro C, Barroso FO, Prashara A, Tentler DP, Yeh H-Y, Tresch MC.** Coordination amongst quadriceps muscles suggests neural regulation of internal joint stresses, not simplification of task performance. *Proc Natl Acad Sci U S A* 117: 201916578, 2020. https://doi.org/10.1073/pnas.1916578117
57. **Avrillon S, Del Vecchio A, Farina D, Pons JL, Vogel C, Umehara J, Hug F.** Individual differences in the neural strategies to control the lateral and medial head of the quadriceps during a mechanically constrained task. *J Appl Physiol* 130: 269-281, 2021.

https://doi.org/10.1152/japplphysiol.00653.2020

Figure Legends

Figure 1. *Experimental setup*. **A**: Participants performed a series of isometric steady contractions at 10% and 30% of the maximum voluntary force with the knee joint fixed at a flexion angle of 45°. **B**. The electromyographic signal of the vastus lateralis (red) and vastus medialis (blue) was recorded using two grids of 64 electrodes each and decomposed to study the behaviour of individual motor units.

Figure 2. *Representative Profiles of IMC*. **A:** Smoothed discharge rate of eleven motor units identified in the vastus lateralis within the 30-second portion of a 30% MVF steady contraction performed by a representative participant. Force is depicted in black. **B:** Examples of individual coherence profiles for each lower limb of the ACLR (Reconstructed and Contralateral) and Control (Dominant and Non Dominant) groups for increasing pairs of MUs considered in the analysis of the VL muscle. **C:** Examples of individual coherence profiles for each lower limb of the ACLR (Reconstructed and Contralateral) and Control (Dominant and Non Dominant) groups for increasing pairs of MUs considered in the analysis of the VM muscle.

Figure 3. *Differences in motor unit discharge rate (MU DR) and inter-spike interval variability (CovISI)*. **Upper panels:** Distribution of DR values for all valid Mus that have been identified for each muscle and lower limb through HDsEMG decomposition. **Lower panels**: Distribution of CovISI values for all valid MUs that have been identified for each muscle and lower limb through HDsEMG decomposition. MU values are represented using different color-filled circles for each lower limb. The mean and SD are reported for each lower limb.

Figure 4. *Profiles of IMC*. **A.** Mean IMC across MUs of the vastus lateralis (VL) identified during a sustained contraction at 10% MVF. **B.** Mean IMC across MUs of the vastus medialis (VM) identified during a sustained contraction at 10% MVF. **C.** Mean IMC across MUs of the VL identified during a sustained contraction at 30% MVF. **D.** Mean IMC across MUs of the VM identified during a sustained contraction at 30% MVF. Individual profiles are depicted for both groups within each of the upper panels (**A-D**). The shaded areas represent the standard error. **E.** Individual values of IMC within the Delta (0-5 Hz) band during contractions at 10% and 30% of the MVF, displayed for both VL and VM. **F.** Individual values of IMC within the Alpha (6-12 Hz)

band during contractions at 10% and 30% of the MVF, displayed for both VL and VM. **G** Individual values of IMC within the Beta (15-30 Hz) band during contractions at 10% and 30% of the MVF, displayed for both VL and VM. Lower limb means ± SD are represented using white (ACLR group) and grey (CONTROL group) bar plots. Participant-specific values are represented using different color-filled circles for each lower limb. * $P<0.05$

Figure 5. *Proportion of common input at 10% of MVF.* Relationships between the mean values of delta coherence (0–5 Hz) and the number of motor units identified in the vastus lateralis (VL) and vastus medialis (VM) for each side and participant. The lower panels show the standard deviation (SD) across participants. These relationships were fitted by least-squares and the proportion of common input (PCI) with respect to the total input to pool of motor neurons was computed as the slope for each participant. Right panels show mean ± SD of the PCI of each lower limb. * $P<0.05$

Figure 6. *Proportion of common input at 30% of MVF.* Relationships between the mean values of delta coherence (0–5 Hz) and the number of motor units identified in the vastus lateralis (VL) and vastus medialis (VM) for each side and participant. The lower panels show the standard deviation (SD) across participants. These relationships were fitted by least-squares and the proportion of common input (PCI) with respect to the total input to pool of motor neurons was computed as the slope for each participant. Right panels show mean ± SD of the PCI of each lower limb. * $P<0.05$

Figure 7. Proportions of *motor unit modes*. **A-B.** Coefficients (ranging from -1 to 1) between the discharge rate of MUs and *muscle modules* are represented for each lower limb of the ACLR (Reconstructed and Contralateral, A panel) and Control (Dominant and Non Dominant, B panel) groups, using green lines for the VL and violet lines for the VM. Grey dots indicate shared module spaces. Note that few motor units, blue (VM) and red (VL) dots, were associated with the other *muscle module*. **C-D-E.** Overall proportions of *Self* (A), *Mixed* (B) *and Other* (C) *motor unit modes*. Lower limb means ± SD are reported for each cluster of motor units. *$P < 0.05$.

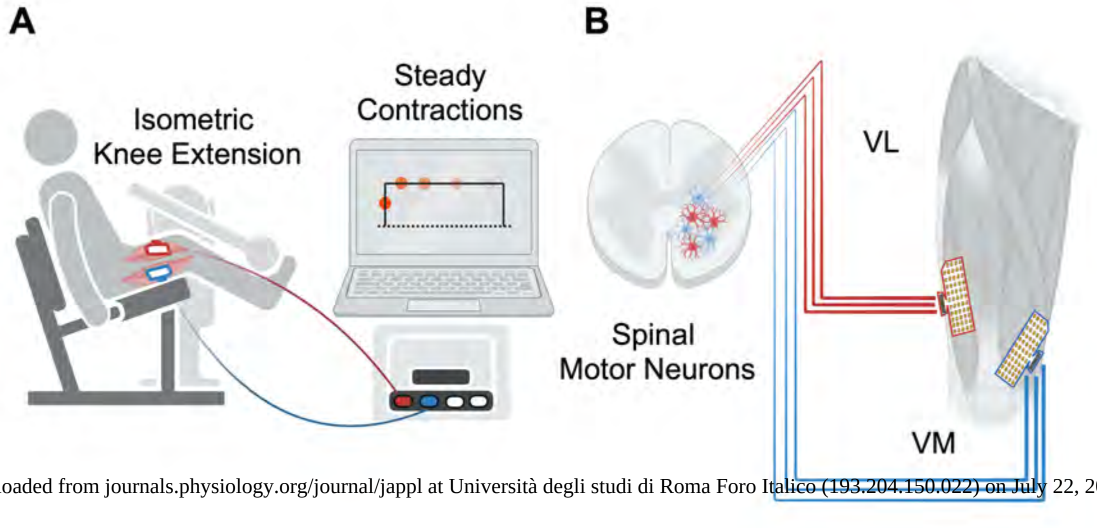
A
Isometric
Knee Extension
Steady
Contractions
B
VL
Spinal
Motor Neurons
VM

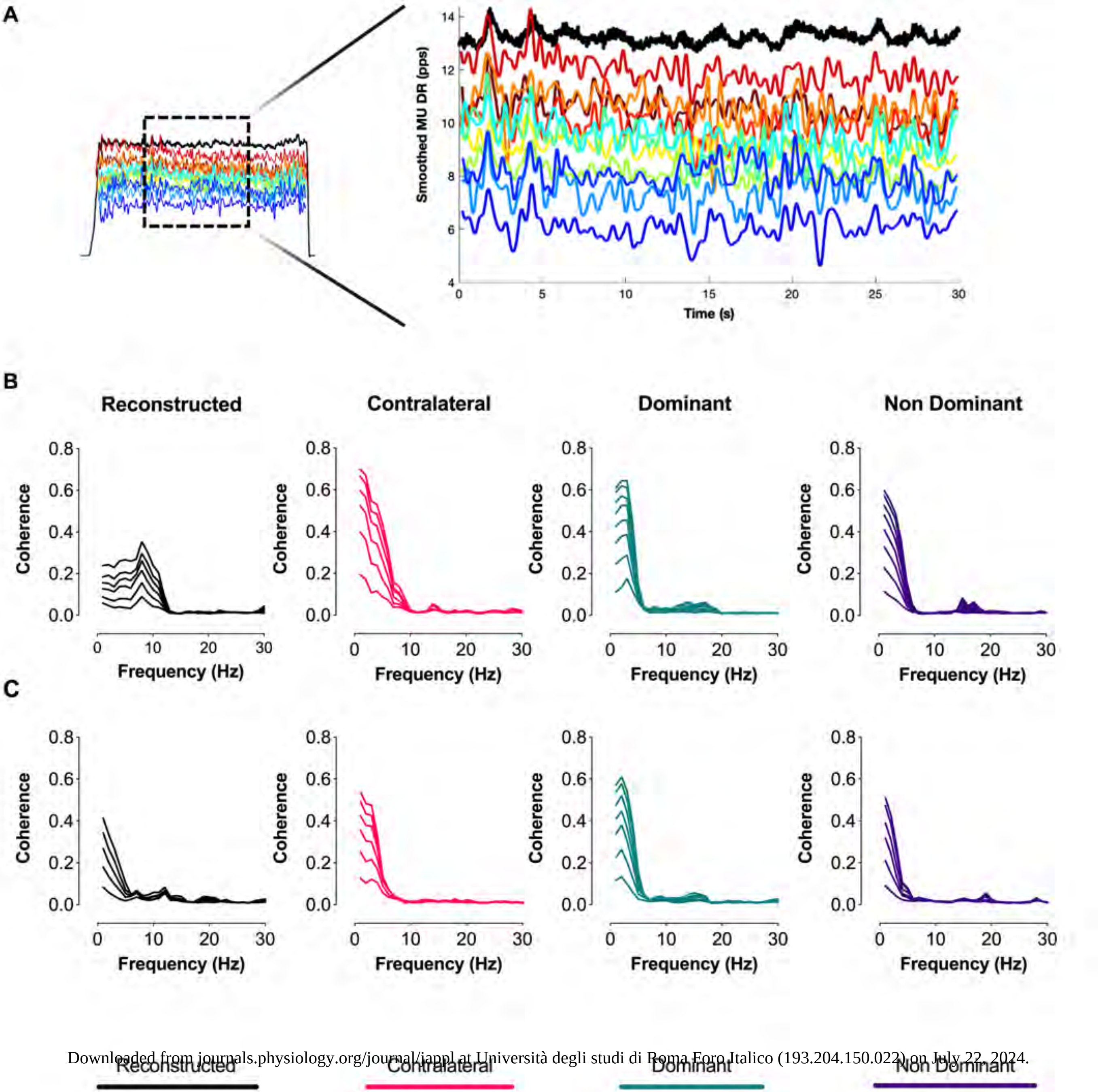
A
Smoothed MU DR (pps)
Time (s)
B
Reconstructed
Contralateral
Dominant
Non Dominant
Coherence
Frequency (Hz)
C
Reconstructed
Contralateral
Dominant
Non Dominant

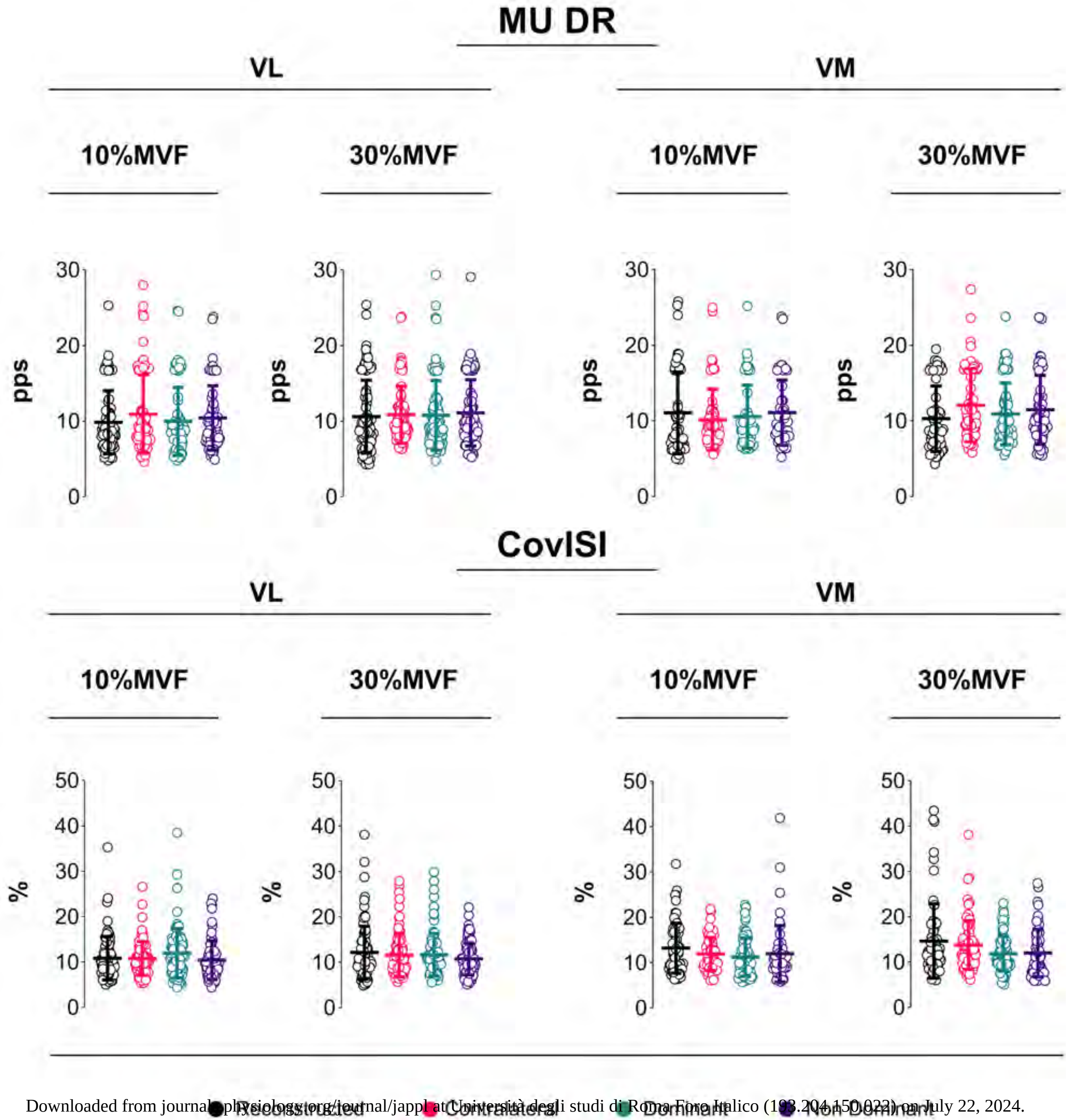
MU DR
VL
VM
10%MVF
30%MVF
10%MVF
30%MVF
pps
CovISI
VL
VM
10%MVF
30%MVF
10%MVF
30%MVF
%
Reconstructed
Contralateral
Dominant
Non Dominant

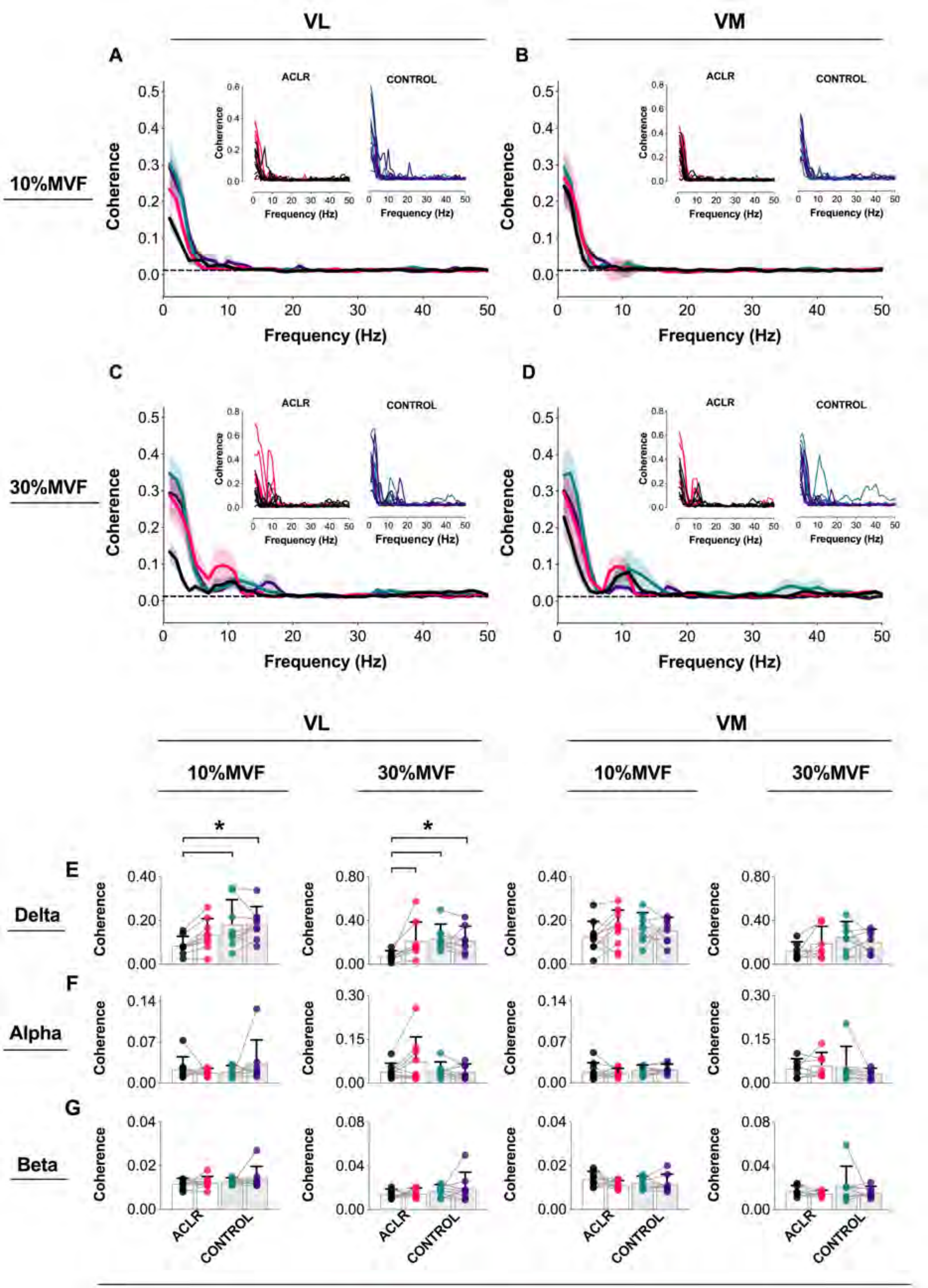

VL
VM
A
B
10%MVF
ACLR
CONTROL
Coherence
Frequency (Hz)
C
D
30%MVF
VL
VM
10%MVF
30%MVF
10%MVF
30%MVF
E
Delta
F
Alpha
G
Beta
ACLR
CONTROL
Reconstructed
Contralateral
Dominant
Non Dominant

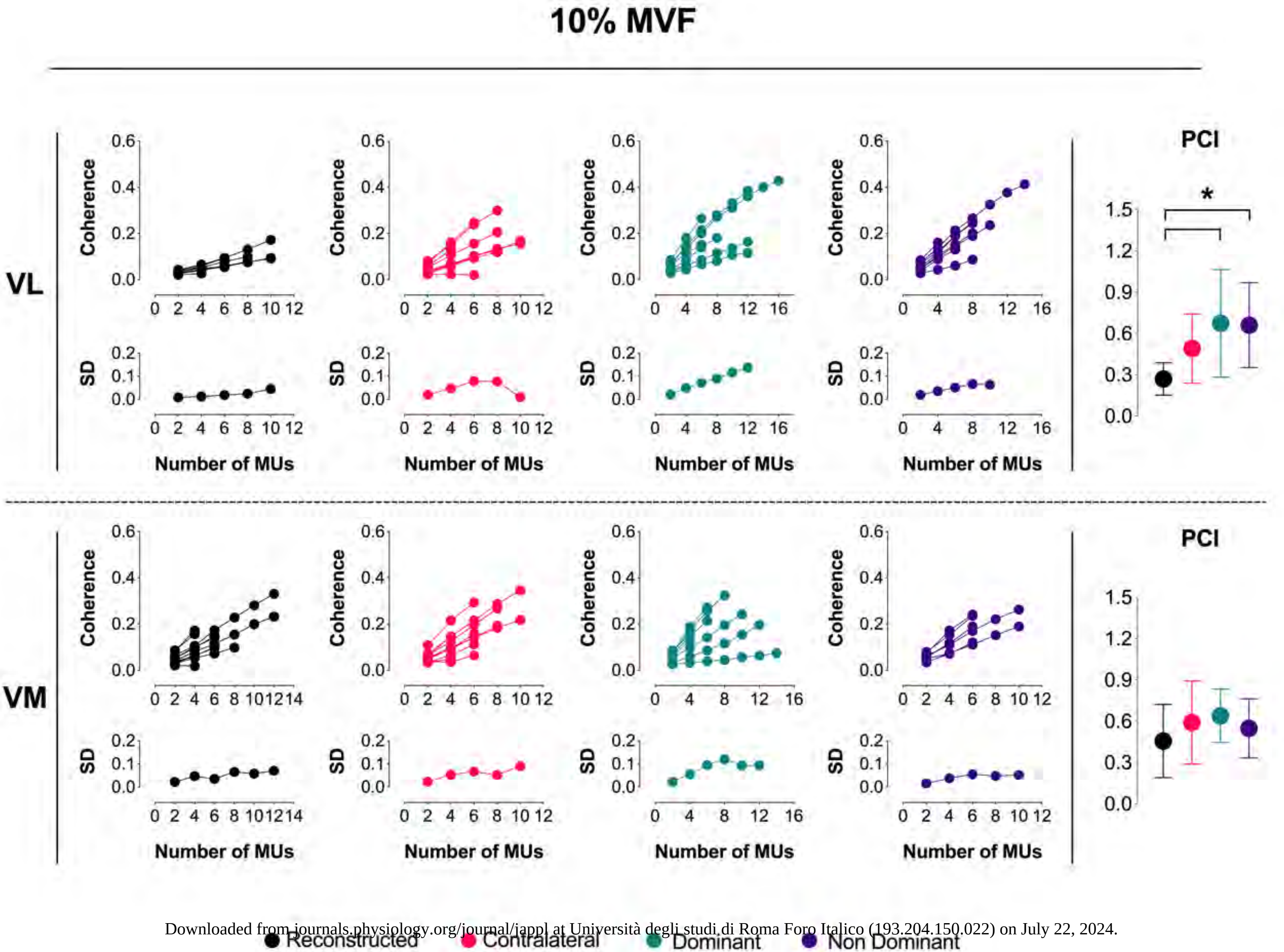

10% MVF
VL
VM
Coherence
SD
Number of MUs
PCI
*
Reconstructed
Contralateral
Dominant
Non Dominant

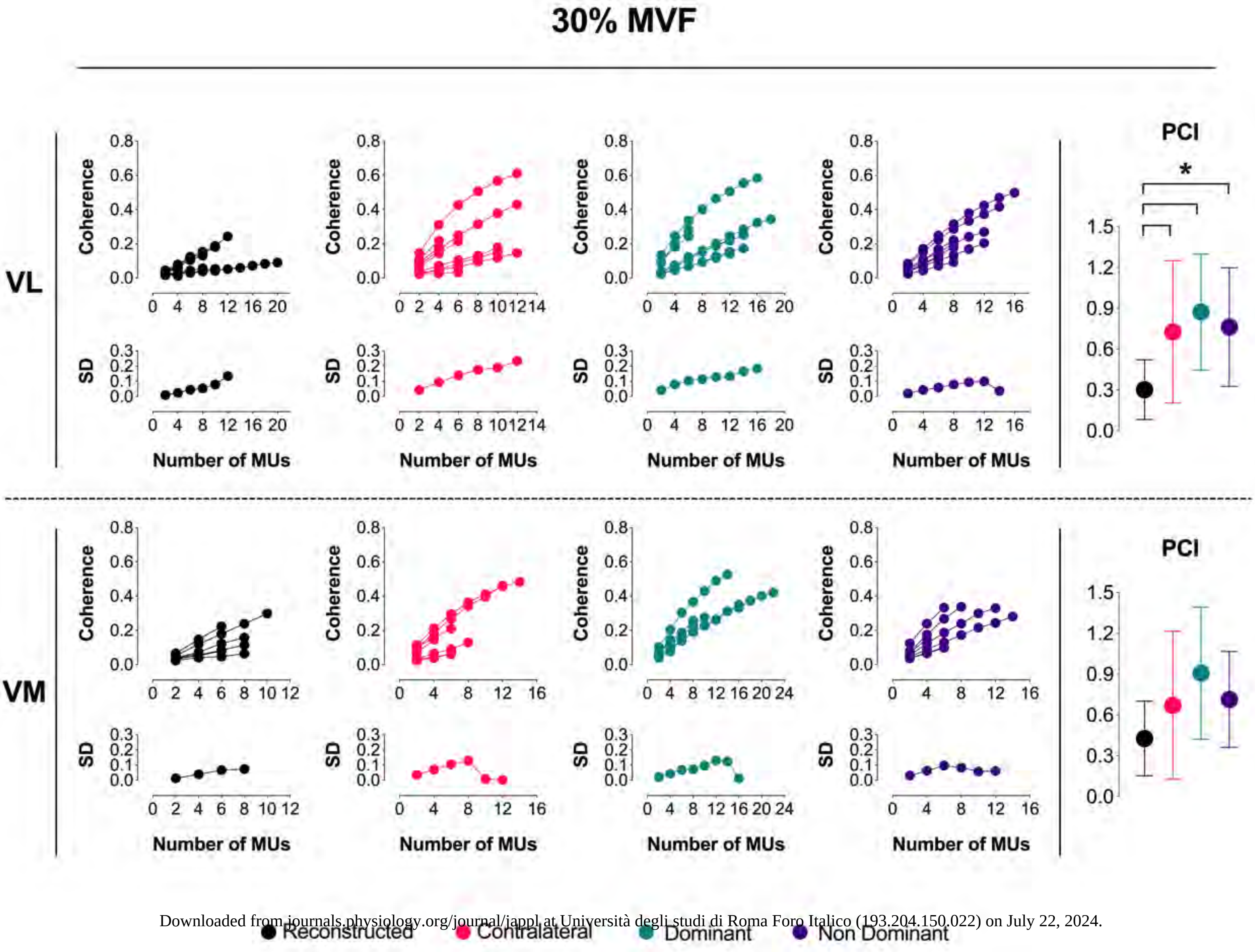

30% MVF
VL
VM
Coherence
SD
Number of MUs
PCI
*
Reconstructed
Contralateral
Dominant
Non Dominant

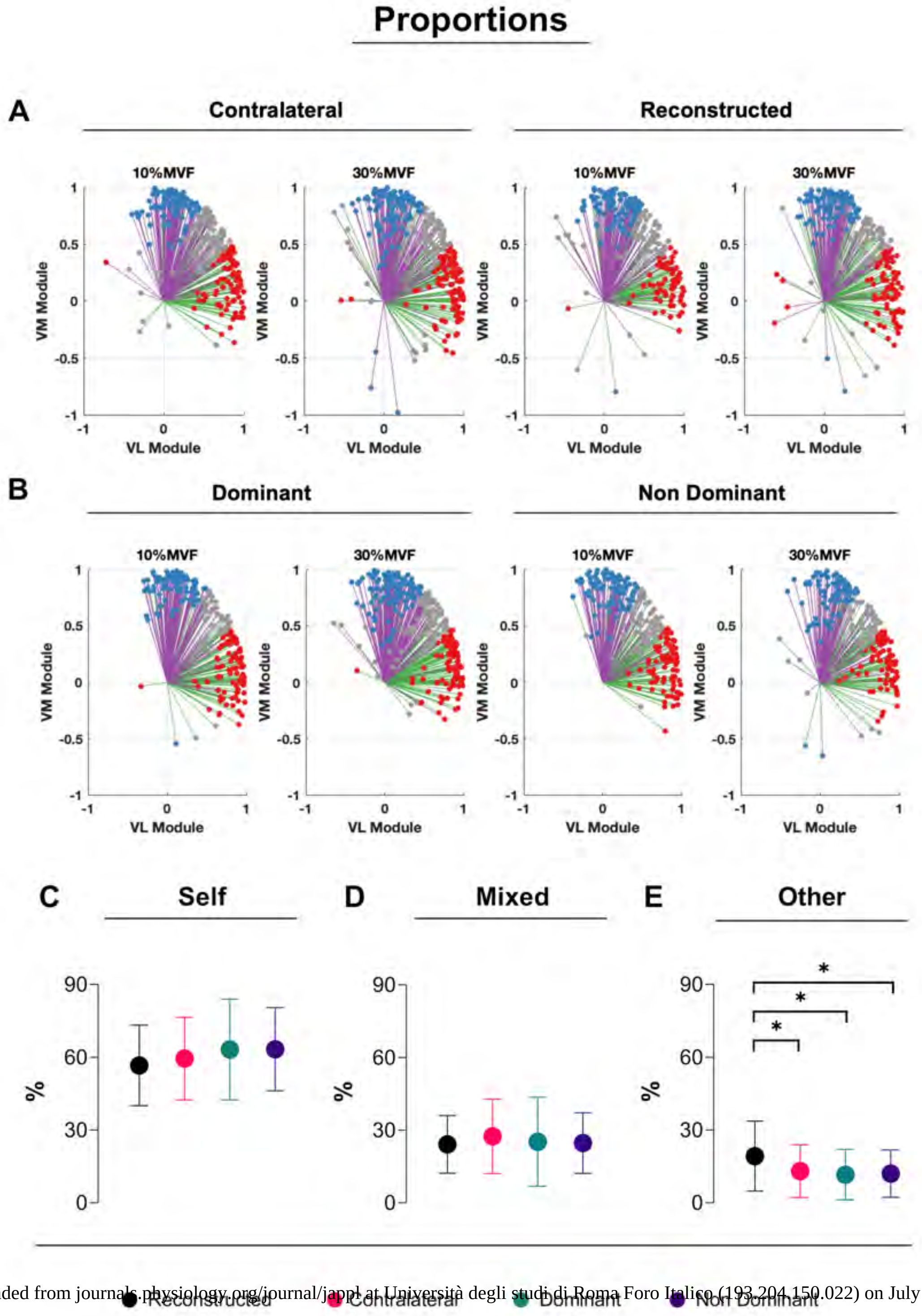
Proportions
A
Contralateral
Reconstructed
10%MVF
30%MVF
VM Module
VL Module
B
Dominant
Non Dominant
C
Self
D
Mixed
E
Other
%
*
Reconstructed
Contralateral
Dominant
Non Dominant

Table 1*. Descriptive characteristics*

Characteristics	Group		P value
	ACLR *(n=11)*	**CONTROL** *(n=9)*	
Age (y)	24.8 ± 3.0	25.7 ± 2.5	.51
BMI (kg·m^{-2})	23.3 ± 0.6	22.9 ± 0.5	.09
Tegner Activity Level score (range: 1-10)	7.7 ± 1.0	7.9 ± 1.1	.73
sCKRS score (range: 0-100)	92.8 ± 2.9	100 ± 0	< 0.001 *
MVF (N)	Reconstructed: 632.7 ± 167.2; Contralateral: 797.4 ± 142.1	Dominant: 638.2 ± 106.3; Non Dominant: 651.1 ± 138.5	< 0.01 #
Graft	BPTB (n=8/10) STGR (n=3/10)	NA	NA
Concomitant Injuries	No other injuries (n=9/10) Meniscus medialis (n=2/10)	NA	NA
Time after ACL surgery (days)	249.9 ± 82	NA	NA

BMI = Body Mass Index; sCKRS= Modified Subjective Cinccinati Knee Rating Scale; BPTB=Bone-Patellar Tendon-Bone graft; MVF= Maximal Voluntary Force; NA = Not Applicable; ***** *significantly different;* **#** *Reconstructed side significantly lower than Contralateral side. Data are reported as mean ± standard deviation.*

Neuroplastic adaptations in common synaptic inputs to motor neurons controlling knee extension forces after ACL reconstruction